Reactions of Iridium and Rhodium Complexes Containing η^2-Benzyne, η^2-Tetrafluorobenzyne, and η^2-Trifluorobenzyne Ligands. Differential Rates of Arene Elimination by Protonation of Isomeric Fluoroaryl Complexes and Restricted Rotation of PMe_3 Ligands in *ortho*-Iodo and *ortho*-Bromoaryl Complexes

Russell P. Hughes,*,† Roman B. Laritchev,† Alex Williamson,†
Christopher D. Incarvito,‡ Lev N. Zakharov,‡ and Arnold L. Rheingold‡

Departments of Chemistry, 6128 Burke Laboratory, Dartmouth College, Hanover, New Hampshire 03755, and University of Delaware, Newark, Delaware 19716

Received January 22, 2003

Treatment of the tetrafluorobenzyne complex Cp*Ir(η^2-C_6F_4)(PMe_3) (**1**) with $MeCO_2H$ affords the tetrafluorophenyl complex Cp*Ir(2,3,4,5,-C_6F_4H)(PMe_3)(O_2CMe) (**2**), which, on treatment with $NaBH_4$, affords the hydride complex Cp*Ir(2,3,4,5,-C_6F_4H)(PMe_3)H (**3**). Treatment of **3** with *n*-BuLi affords the trifluorobenzyne complex Cp*Ir(3,4,5-C_6F_3H)(PMe_3) (**4**). Treatment of **4** with $MeCO_2H$ gives a mixture of two protonation products, Cp*Ir(2,3,4-$C_6F_3H_2$)(PMe_3)(O_2CMe) (**5**) and Cp*Ir(3,4,5-$C_6F_3H_2$)(PMe_3)(O_2CMe) (**6**) in an 8:1 ratio. Treatment of the **5**/**6** mixture with CF_3CO_2H affords 1,2,3-$C_6F_3H_3$ and Cp*Ir(O_2CCF_3)$_2$(PMe_3) but at dramatically different rates, with **5** reacting significantly faster than **6**. Treatment of **1a** with Br_2, I_2, or MeI gives the oxidative addition products Cp*Ir(2-C_6BrF_4)Br(PMe_3) (**7**), Cp*Ir(2-C_6IF_4)I(PMe_3) (**8**), or Cp*Ir(2-C_6MeF_4)I(PMe_3) (**9**), respectively. The variable-temperature proton NMR spectra of complexes **7** and **8** reveal an unusual restricted rotation about the Ir−PMe_3 bonds on the NMR time scale (**7**, $\Delta G^{\ddagger} = 39 \pm 2$ kJ mol^{-1}; **8**, $\Delta G^{\ddagger} = 38 \pm 2$ kJ mol^{-1}). Similarly, treatment of Cp*Rh(η^2-C_6F_4)(PMe_3) (**1b**) with I_2 leads to formation of Cp*Rh(2-C_6IF_4)I(PMe_3) (**10**), which also exhibits restricted rotation about the metal−phosphorus bond ($\Delta G^{\ddagger} = 44 \pm 2$ kJ mol^{-1}). While the tetrafluorobenzyne complex (**1a**) is unreactive toward CO, the hydrocarbon analogue Cp*Ir(η^2-C_6H_4)(PMe_3) (**1c**) does react to give the CO monoinsertion product (**11**). Compound **1c** also reacts with I_2 to afford Cp*Ir(2-C_6IH_4)I(PMe_3) (**12**), which also shows restricted rotation about the Ir−PMe_3 bond ($\Delta G^{\ddagger} = 43 \pm 2$ kJ mol^{-1}). X-ray crystal structures of complexes **3**, **4**, **5**, **7**, **8**, **10**, and **11** are reported.

Introduction

There are many examples of transition metal complexes containing the benzyne (η^2-C_6H_4) ligand, and their reaction chemistry has been studied extensively.[1−4] With the exception of complexes of the type Re(η^2-C_6H_3-Me)(2-MeC_6H_4)$_2$(PMe_2R)$_2$]$^+$, their neutral precursors,[5] and Ta(η^2-C_6H_4)Cp($C_2B_4H_4Et_2$)(PMe_3),[6] which are remarkably unreactive, early transition metal complexes of benzyne have been shown to undergo a rich insertion chemistry with substrates such as alkenes, alkynes, ketones, nitriles, CO, CO_2, CS_2, and even metal carbonyl complexes.[2] These insertions are often regioselective and lead to a large variety of new metallacycles and organic compounds. Zirconium-benzyne complexes in particular have been used extensively in organic synthesis.[7,8] Late transition metal benzyne complexes have also been thoroughly studied and shown to have a rich insertion chemistry.[3,9,10]

We have described previously the syntheses and molecular structures of tetrafluorobenzyne complexes of iridium (**1a**) and rhodium (**1b**) and the analogous benzyne complex of iridium (**1c**).[11,12] Here we report

* Corresponding author.
† Dartmouth College.
‡ University of Delaware.

(1) Retbøll, M.; Edwards, A. J.; Rae, A. D.; Willis, A. C.; Bennett, M. A.; Wenger, E. *J. Am. Chem. Soc.* **2002**, *124*, 8348−8360.
(2) Bennett, M. A.; Schwemlein, H. P. *Angew. Chem., Int. Ed. Engl.* **1989**, *28*, 1296−1320.
(3) Bennett, M. A.; Wenger, E. *Chem. Ber./Recl.* **1997**, *130*, 1029−1042.
(4) Jones, W. M.; Klosin, J. *Adv. Organomet. Chem.* **1998**, *42*, 147−221.
(5) Arnold, J.; Wilkinson, G.; Hussain, B.; Hursthouse, M. B. *Organometallics* **1989**, *8*, 415−420.
(6) Houseknecht, K. L.; Stockman, K. E.; Sabat, M.; Finn, M. G.; Grimes, R. N. *J. Am. Chem. Soc.* **1995**, *117*, 1163−1164.
(7) Buchwald, S. L.; Nielsen, R. B. *Chem. Rev.* **1988**, *88*, 1047−1058.
(8) Broene, R. D.; Buchwald, S. L. *Science* **1993**, *261*, 1696.
(9) Hartwig, J. F.; Bergman, R. G.; Andersen, R. A. *J. Am. Chem. Soc.* **1991**, *113*, 3404−3418.
(10) Hartwig, J. F.; Andersen, R. A.; Bergman, R. G. *J. Am. Chem. Soc.* **1989**, *111*, 2717−2719.

10.1021/om030048w CCC: $25.00
Publication on Web 03/29/2003

some examples of their reaction chemistry.

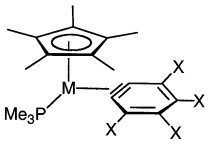

1a M = Ir; X = F
1b M = Rh; X = F
1c M = Ir; X = H

Results and Discussion

Transition metal benzyne complexes, particularly those of late transition metals, such as Ni(η^2-C_6H_4)(Cy_2-$PCH_2CH_2PCy_2$)[2,13] and Ru(η^2-C_6H_4)(PMe_3)$_4$,[9,10] have been shown to undergo addition reactions with a variety of electrophiles such as acids, alcohols, amines, CH_3-CN, H_2O, I_2, and MeI. In each case, addition across the M−C(η^2-benzyne) bond occurs to give an *ortho*-substituted phenyl complex. Only the unusual complexes [Re(η^2-C_6MeH_3)(2-MeC_6H_4)$_2$(PMe_2R)$_2$]$^+$ and their neutral precursors[5] appear to be unreactive to electrophiles, even including excess CF_3SO_3H.

Treatment of Cp*Ir(η^2-C_6F_4)(PMe_3) (**1a**) with either 1 equiv or an excess of acetic acid produces the expected addition product Cp*Ir(2,3,4,5-C_6F_4H)(PMe_3)(O_2CMe) (**2**). Presumably, the reaction proceeds by protonation of one of the equivalent coordinated benzyne carbon atoms to give an aryl ring, followed by trapping of the acetate anion by the metal center. Notably, even a large excess of acetic acid does not cause protonation of the Ir−aryl bond to afford free arene.

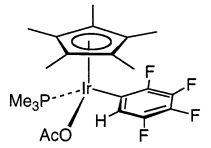

2

Treatment of **2** with $NaBH_4$ produces the analogous hydride complex Cp*Ir(2,3,4,5-C_6F_4H)(PMe_3)H (**3**). The ^{1}H, ^{19}F, and ^{31}P{^{1}H} NMR spectra of **3** are broad at room temperature. On cooling to −40 °C, the broad resonances separate into two sets of sharp resonances in a ratio of 2.3:1, corresponding to two rotamers about the Ir−C_6F_4H bond. It is of interest to note that the Ir−H resonance in the ^{1}H NMR spectrum of the major isomer **3a** appears as a doublet coupled only to ^{31}P ($^2J_{HP}$ = 35.5 Hz), while the analogous Ir−H resonance of the minor isomer **3b** appears as a doublet of doublets with an additional coupling to the *ortho*-fluorine atom ($^2J_{HP}$ = 37.5 Hz, $^4J_{HF}$ = 12.5 Hz). This strongly suggests that,

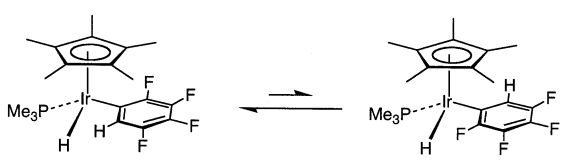

3a **3b**

in the minor isomer **3b**, the *ortho*-fluorine atom on the C_6F_4H ring is oriented toward the hydride ligand. In related fluoroaryl(hydrido) complexes we have previously used ^{1}H/^{19}F HOESY spectroscopy to show that the fluorine closer to the hydride ligand or to the PMe_3 ligand is the one that couples more strongly to ^{1}H or ^{31}P, respectively.[12] Therefore, in the major isomer **3a**, the *ortho*-fluorine should be oriented toward the PMe_3 ligand. Indeed, the ^{31}P{^{1}H} resonance of the major isomer appears as a doublet with coupling to the *ortho*-fluorine ($^4J_{PF}$ = 5 Hz), while that of the minor isomer appears as a singlet. The major isomer **3a** observed in solution is also that observed in the solid state (see below).

As observed previously for other fluoroaryl(hydrido) complexes,[11,12] treatment of **3** with excess *n*-BuLi produces the expected trifluorobenzyne complex Cp*Ir(η^2-3,4,5-C_6F_3H)(PMe_3) (**4**). The ethyl(tetramethyl)cyclopentadienyl analogue of **4** has been reported previously and shows restricted rotation about the Ir−benzyne bond.[12] Treatment of **4** with acetic acid produces a mixture of two compounds, Cp*Ir(2,3,4-$C_6F_3H_2$)(PMe_3)(O_2-CMe) (**5**) and Cp*Ir(3,4,5-$C_6F_3H_2$)(PMe_3)(O_2CMe) (**6**), in a ratio of 8:1. Evidently, the two inequivalent *ipso*-carbon atoms on the benzyne ligand are protonated at different rates. The preference for attack at the *ipso*-carbon that is *ortho* to the ring carbon bearing hydrogen may be due to a difference in charge distribution on the unsymmetrical η^2-C_6F_3H ligand. The ^{19}F NMR spectrum of the minor product **6** consists of a triplet of triplets at −171.9 ppm ($^3J_{FF}$ = 20.0 Hz, $^4J_{FH}$ = 8.0 Hz), corresponding to the *para*-fluorine atom, and a broad singlet at −141.4 ppm, corresponding to the *meta*-fluorine atoms. On cooling a solution of the **5**/**6** mixture in CD_2-Cl_2 to −75 °C, the broad peak at −141.4 ppm broadens further, virtually disappearing at −35 °C, and then separates into two separate broad peaks at −141.3 and −139.9 ppm, indicating slowing of rotation about the Ir−$C_6F_3H_2$ bond. While no attempts were made to separate the mixture of **5** and **6** in bulk, a crystal of pure **5** was obtained and characterized by X-ray diffraction (see below).

In contrast to the lack of reactivity with acetic acid, treatment of the **5**/**6** mixture with excess trifluoroacetic acid resulted in cleavage of the Ir−aryl bonds to produce 1,2,3-$C_6F_3H_3$.[14] The iridium product was the bis-trifluoroacetate complex Cp*Ir(O_2CCF_3)$_2$(PMe_3), which was isolated and characterized. Analogous treatment with CF_3CO_2D resulted in formation of C_6-1,2,3-F_3-4-DH_2 as the major organic product (identified by three inequivalent fluorine resonances in the ^{19}F NMR spectrum. The corresponding organic product, C_6-1,2,3-F_3-5-DH_2, produced by reaction of the minor isomer (**6**) with CF_3-CO_2D, was not observed by NMR, probably due to masking by the resonances of the major organic product. Interestingly, the relative rates of reaction of **5** and **6** with excess CF_3CO_2H in CD_2Cl_2 solution appear to be significantly different. Within 5 min, complex **5** was completely converted to 1,2,3-$C_6F_3H_3$ and Cp*Ir(O_2-CCF_3)$_2$(PMe_3), but a significant amount of **6** remained unreacted even after 2 h. Only after about 24 h was complex **6** completely consumed. The large difference

(11) Hughes, R. P.; Williamson, A.; Sommer, R. D.; Rheingold, A. L. *J. Am. Chem. Soc.* **2001**, *123*, 7443−7444.

(12) Hughes, R. P.; Laritchev, R. B.; Williamson, A.; Incarvito, C. D.; Zakharov, L. N.; Rheingold, A. L. *Organometallics* **2002**, *21*, 4873−4885.

(13) Bennett, M. A.; Hambley, T. W.; Roberts, N. K.; Robertson, G. B. *Organometallics* **1985**, *4*, 1992−2000.

(14) Ernst, L.; Wray, V. *J. Magn. Reson.* **1977**, *28*, 373−375.

Scheme 1

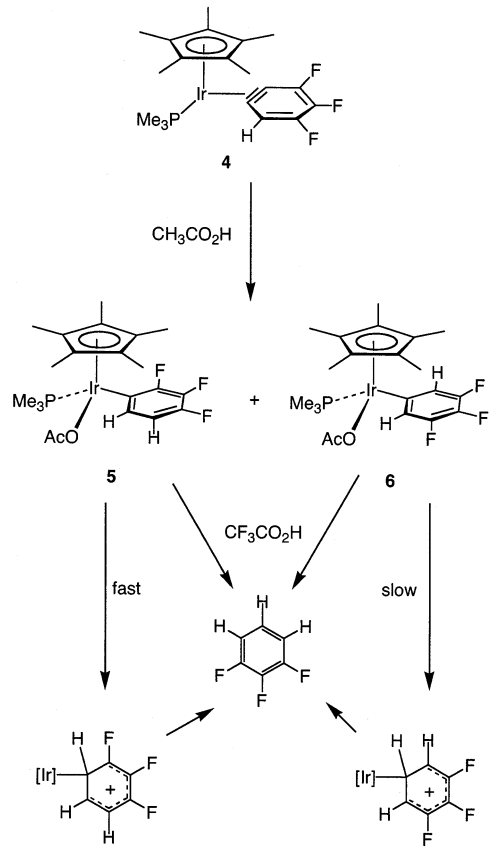

in rates may be due to the effects of π-donor fluorine stabilization on the relative stabilities of the intermediate protonated complexes as shown in Scheme 1, assuming that the mechanism of arene elimination is effectively an electrophilic aromatic substitution reaction. The putative carbocation obtained from **5** has fluorines in the *ortho*- and *para*-positions relative to the site of protonation, while that derived from **6** has only one stabilizing π-donor fluorine in the *para*-position. This interpretation may be simplistic, as it takes into consideration only the stability of the Wheland intermediates and ignores possible differences in activation energy barriers, but it provides a satisfying qualitative rationale.

Treatment of **1a** with Br_2 or I_2 affords the corresponding addition products Cp*Ir(2-C_6BrF_4)Br(PMe_3) (**7**) and Cp*Ir(2-C_6IF_4)I(PMe_3) (**8**). The ^1H, ^{19}F, and ^{31}P NMR spectra of **7** show two isomers in a ratio of 9:1 at 35 °C. The $^{31}P\{^1H\}$ NMR spectrum of the major isomer appears as a doublet with a large coupling to the *ortho*-fluorine on the aryl ring ($^4J_{PF} = 31.7$ Hz), while that of the minor isomer appears only as a singlet. By analogy to previous arguments (vide supra) the two isomers are rotamers about the Ir−C_6BrF_5 bond, with the major isomer corresponding to rotamer **7a**, in which the *ortho*-fluorine

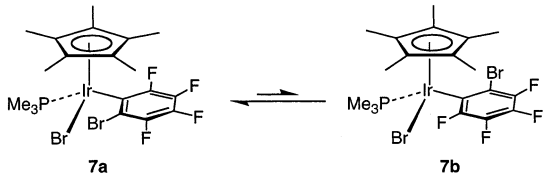

substituent is directed more closely toward the PMe_3 ligand. X-ray structural analysis (see below) shows this conformation in the solid state. At room temperature, the ^1H, ^{19}F, and ^{31}P NMR spectra of **7a** are sharp and well resolved, except for the ^1H NMR resonance corresponding to the methyl groups on phosphorus, which appears as a broad hump. Warming a CD_2Cl_2 solution of **7a/7b** to 35 °C results in a sharpening of the PMe_3 resonance of **7a** to the expected doublet of doublets ($^2J_{HP} = 10.5$ Hz, $^6J_{HF} = 1.5$ Hz). The corresponding resonance of **7b** could not be observed, presumably due to overlap with other resonances. However, on stepwise cooling to −80 °C, the broad PMe_3 resonance broadens further, disappears into the baseline, and then reappears as three separate resonances in a ratio of 3:3:3. Two of the resonances appear as doublets due to coupling to ^{31}P and the other as a doublet of doublets due to additional coupling to the *ortho*-fluorine ($^2J_{HP} = 9.5$ Hz, $^6J_{HF} = 3.5$ Hz). Analogous observations of the resonances of **7b** were not possible due to the low concentration of this isomer. These data are consistent only with slowing of rotation about the Ir−PMe_3 bond to produce three separate environments for the methyl groups. At −80 °C, one of these environments is evidently located in closer proximity to the *ortho*-fluorine atom than the other two, resulting in a significant H−F coupling constant, approximately 3 times larger than the site exchange averaged coupling observed at 35 °C. There are several reports of restricted rotation about M−P bonds in phosphine complexes of transition metals. This phenomenon has been observed for PMe_2Ph,[15−17] PPh_3,[18,19] and PEt_3[20] ligands, but to our knowledge has not been observed previously for PMe_3. Using line shape analysis of the spectra of **7a**, the free energy of activation ($\Delta G^{\ddagger}$) for rotation about the Ir−PMe_3 bond was calculated to be 39 ± 2 kJ/mol. In contrast to the behavior of the PMe_3 resonance, the two Cp* resonances for **7a** and **7b** do not coalesce at 35 °C, indicating a significant barrier to rotation about the Ir−aryl bond.

The corresponding iodo complex **8** exists as only one observable isomer, and the $^{31}P\{^1H\}$ resonance appears as a doublet with a large P−F coupling constant ($^4J_{PF} = 38.3$ Hz), indicating that the *ortho*-fluorine is proximal to the PMe_3 ligand, as shown and as observed in the solid state structure of **8** (see below). The ^1H NMR spectrum of complex **8** also shows broad resonances corresponding to the PMe_3 ligand, which separate into three separate resonances on cooling to −75 °C. The value of $\Delta G^{\ddagger}$ for rotation about the Ir−PMe_3 bond in **8** was calculated to be 39 ± 2 kJ/mol.

Addition of 1 equiv of I_2 to the rhodium benzyne complex Cp*Rh(η^2-C_6F_4)(PMe_3) (**1b**) affords the expected addition product Cp*Rh(2-C_6IF_4)I(PMe_3) (**9**). Like the analogous iridium complex, **9** exhibits restricted rotation

(15) Lyons, L. J.; Anderson, L. L.; Crane, R. A.; Treichel, P. M. *Organometallics* **1991**, *10*, 587−591.
(16) Deeming, A. J.; Doherty, S.; Marshall, J. E. *Polyhedron* **1991**, *10*, 1857−1864.
(17) Li, L.; Decken, A.; Sayer, B. G.; McGlinchey, M. J.; Bregaint, P.; Thepot, J. Y.; Toupet, L.; Hamon, J. R.; Lapinte, C. *Organometallics* **1994**, *13*, 682−689.
(18) Chudek, J. A.; Hunter, G.; MacKay, R. L.; Kremminger, P.; Schlogl, K.; Weissensteiner, W. *J. Chem. Soc., Dalton Trans.* **1990**, 2001−2005.
(19) Chudek, J. A.; Hunter, G.; MacKay, R. L.; Farber, G.; Weissensteiner, W. *J. Organomet. Chem.* **1989**, *377*, C69−C72.
(20) Crocker, C.; Goodfellow, R. J.; Gimeno, J.; Uson, R. *J. Chem. Soc., Dalton Trans.* **1977**, 1448−1452.

Table 1. Crystal Data and Summary of X-ray Data Collection

	3	**4**	**5**	**7**	**8**	**10**	**11**
formula	$C_{19}H_{26}F_4IrP$	$C_{19}H_{25}F_3IrP$	$C_{21}H_{29}F_3IrO_2P$	$C_{19}H_{24}Br_2F_4IrP$	$C_{19}H_{24}F_4I_2IrP$	$C_{19}H_{24}F_4I_2PRh$	$C_{20}H_{28}IrOP$
fw	553.57	533.56	593.61	711.37	805.35	716.06	507.59
space group	$P2_1/c$	$P\bar{1}$	$P2_1/n$	$P2_1/c$	$P\bar{1}$	$P\bar{1}$	$P2_1/n$
a, Å	9.3766(2)	8.6507(6)	8.5763(6)	8.5001(4)	8.4708(1)	8.438(4)	8.7308(6)
b, Å	17.2097(2)	9.1369(8)	18.8678(13)	16.2603(8)	10.0492(1)	10.029(5)	24.4873(16)
c, Å	12.5355(2)	12.7089(8)	13.7218(10)	15.4398(8)	14.0363(2)	14.079(6)	9.2704(6)
α, deg	90	90.162(5)	90	90	86.016(1)	85.748(8)	90
β, deg	95.0640(10)	90.871(4)	92.905(2)	91.8590(10)	79.914(1)	79.314(9)	99.7860(10)
γ, deg	90	105.362(4)	90	90	71.818(1)	72.045(7)	90
V, Å^3	2014.94(6)	968.49(12)	2217.6(3)	2132.88(18)	1117.50(2)	1113.5(8)	1953.1(2)
Z	4	2	4	4	2	2	4
D(calcd), g/cm^3	1.825	1.830	1.778	2.215	2.393	2.136	1.726
abs coeff, mm^{-1}	6.740	7.000	6.131	10.118	8.843	3.646	6.920
R(*F*), %[a]	2.25	2.72	3.17	2.76	4.34	2.11	5.02
$R_w(F^2)$, %[a]	6.07	8.36	7.13	7.34	8.17	5.63	11.25
temp, K	173(2)	173(2)	173(2)	173(2)	173(2)	223(2)	100(2)
diffractometer	Siemens P4						
radiation	Mo Kα 0.71073 Å						

[a] Quantity minimized = $R_w(F^2) = \sum[w(F_o^2 - F_c^2)^2]/\sum[(wF_o^2)^2]^{1/2}$; $R = \sum\Delta/\sum(F_o)$, $\Delta = |(F_o - F_c)|$.

about the Rh−P bond, which can be "frozen-out" on cooling to −75 °C. The $^{31}P\{^1H\}$ NMR spectrum appears as a doublet of doublets due to coupling with rhodium ($^1J_{PRh}$ = 142.8 Hz) and with the *ortho*-fluorine substituent ($^4J_{PF}$ = 48.9 Hz). As discussed above, the very large P−F coupling constant corresponds to a short distance between the two atoms. The free energy of activation for rotation about the Rh−PMe_3 bond in **9** was calculated to be 44 ± 2 kJ/mol.

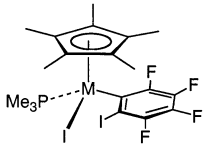

8 M = Ir
9 M = Rh

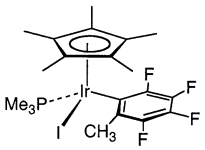

10

In contrast to its rapid reactions with Br_2 and I_2, complex **1a** undergoes reaction with excess MeI only after prolonged heating (110 °C, 84 h). The product is the expected addition product Cp*Ir(2-C_6MeF_4)I(PMe_3) (**10**), for which only one isomer is observed. The $^{31}P\{^1H\}$ resonance appears as a doublet with a large P−F coupling constant ($^4J_{PF}$ = 33.9 Hz). In complex **10**, the PMe_3 resonance in the ^1H NMR spectrum at room temperature is sharp and well resolved into the usual doublet of doublets, indicating a much lower barrier to rotation about the Ir−P bond. Further NMR studies on this complex were not performed.

Unlike most known benzyne complexes, **1a** is remarkably inert to insertion of unsaturated molecules. Prolonged treatment with CO, $CH_2{=}CH_2$, or $CH_2{=}CHCO_2Me$ at 80 °C in benzene solution does not result in any reaction, and the starting material is recovered unchanged. In contrast, the hydrocarbon analogue **1c** does react with CO to afford a monoinsertion product **11**, characterized spectroscopically and crystallographically. As with its tetrafluorobenzyne analogue **1a**, the hydrocarbon complex **1c** also reacts with I_2 to afford an analogous complex **12**. Complex **12** exists in C_6D_6 solution as a 12:1 mixture of rotamers about the Ir−aryl bond, while in CD_2Cl_2 solution the ratio is 5:1. In CD_2Cl_2 both rotamers show restricted rotation about their respective Ir−PMe_3 bonds. The resonances for the individual methyl groups in the PMe_3 ligands of each isomer can be observed at −80 °C, but the decoalescence behavior of the minor isomer could not be observed accurately due to its low concentration. However, the barrier to rotation about the Ir−P bond for the major isomer was calculated by line shape analysis to be 43 ± 2 kJ/mol, a value not significantly different from the other examples described above.

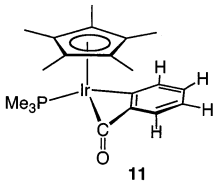

11

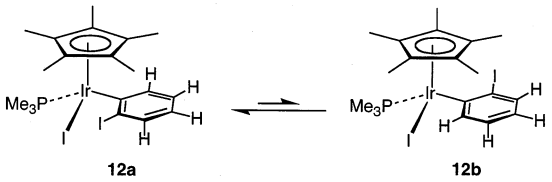

12a **12b**

Crystal Structures

Details of the crystallographic determinations for complexes **3**, **4**, **5**, **7**, **8**, **10**, and **11** are collected in Table 1, and ORTEP diagrams and atom labeling schemes are illustrated in Figures 1−7. Selected distances and angles are collected in Table 2. For the aryl complexes **3**, **5**, **7**, **8**, and **10**, a set of projections viewed down the M−C bond to the aryl ligand is provided in Figure 8. All these compounds show the expected three-legged piano-stool structure. All the structures contain an *ortho*-fluorine on the aryl ring that is proximal to PMe_3, providing a common point of comparison in all cases. Comparison of the structures of **3** and **5** illustrates that replacement of the hydride ligand by acetate is not accompanied by any significant lengthening of the Ir−aryl bond, but does result in significant increases in the Ir−P and Ir−Cp* centroid distances. The other notable change is the canting of the aryl ring away from acetate toward PMe_3, with a dramatic decrease in the P−F(*ortho*) distance from 3.66 to 3.26 Å, as illustrated in Figure 8. As shown in Figure 8, the Ir and the *ipso*- and *para*-carbons of the aryl ring are essentially eclipsed. The degree and direction of aryl ring canting are clearly

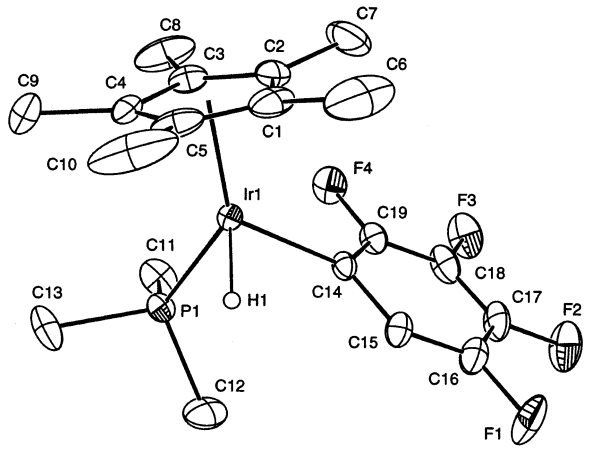

Figure 1. ORTEP plot and atom-numbering scheme for complex **3**. Ellipsoids are shown at the 30% probability level, and H atoms are excluded for clarity, except for H1.

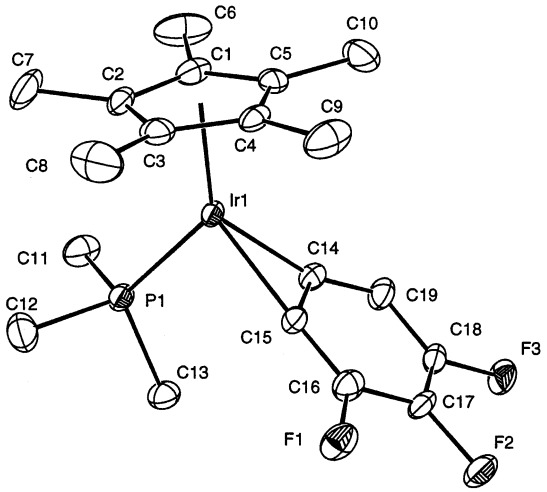

Figure 2. ORTEP plot and atom-numbering scheme for complex **4**. Ellipsoids are shown at the 30% probability level, and H atoms are excluded for clarity. Selected bond distances and angles: Ir1−C14 2.031(6), Ir1−C15 2.049(5), Ir1−P1 2.2412(15), C14−C19 1.349(8), C14−C15 1.356(8), C15−C16 1.332(8), C16−C17 1.393(9), C17−C18 1.348(9), C18−C19 1.379(9): C14−Ir1−C15 38.8(2), C14−Ir1−P1 90.83(17), C15−Ir1−P1 90.60(16), C19−C14−C15 121.2(5), C16−C15−C14 120.6(5), C15−C16−C17 119.4(5), C18−C17−C16 119.8(5), C17−C18−C19 120.2(5), C14−C19−C18 118.7(5).

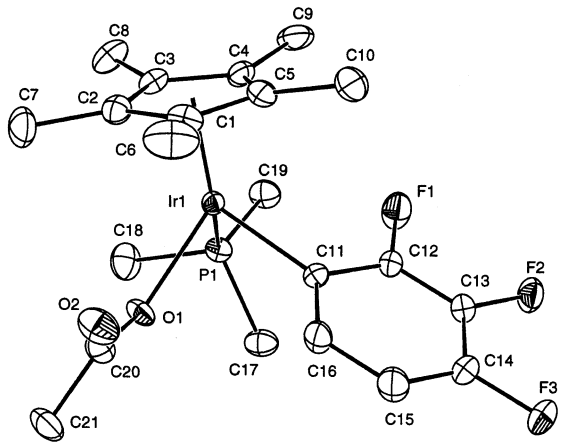

Figure 3. ORTEP plot and atom-numbering scheme for complex **5**. Ellipsoids are shown at the 30% probability level, and H atoms are excluded for clarity.

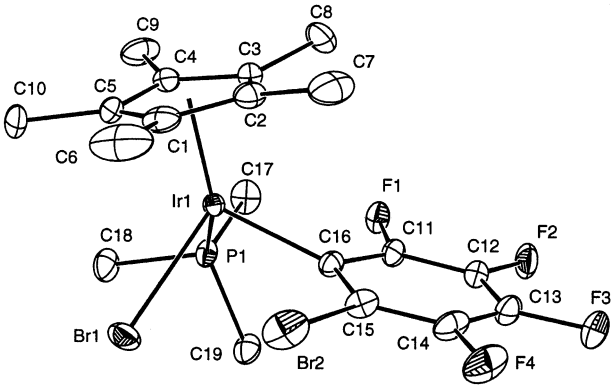

Figure 4. ORTEP plot and atom-numbering scheme for complex **7**. Ellipsoids are shown at the 30% probability level, and H atoms are excluded for clarity.

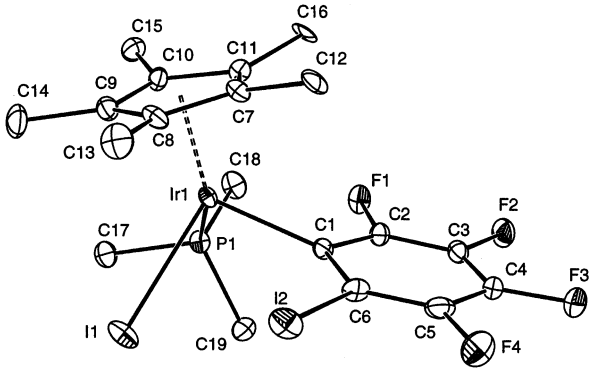

Figure 5. ORTEP plot and atom-numbering scheme for complex **8**. Ellipsoids are shown at the 30% probability level, and H atoms are excluded for clarity.

controlled by the steric interaction between the *ortho*-aryl substituent and its proximal ligand, as has previously been discussed for other fluoroaryl analogues.[12] Introduction of the *ortho*-bromo or -iodo substituents in complexes **7**, **8**, and **10** results in two significant changes, presumably driven by the repulsive interaction between the *ortho*-Br (or I) and its proximal bromo (or iodo) ligand on the metal. The first is an even more pronounced canting of the aryl ring toward PMe_3, and the second is a bending of the aryl such that the *para*-carbon is no longer eclipsed with the metal and the *ipso*-aryl carbon atom, but is displaced toward PMe_3. Both these distortions result in diminished values of the P−F(*ortho*) distances to less than 3 Å, and this increased steric congestion around the PMe_3 ligand is presumably responsible for the increased barrier to rotation about the M−PMe_3 bond observed in solution. Increased steric congestion at the metal center in these three compounds is also revealed by slightly increased M−C(aromatic), M−Cp* centroid, and M−P distances.

The crystal structure of the trifluorobenzyne complex **4** shows no remarkable differences from its tetrafluorobenzyne analogues.[11,12] The *ortho*-fluorine is disordered between the two possible positions. The structure of the CO insertion product **11** likewise contains no remarkable features. Selected bond distances and angles for each compound are included in the figure captions for these structures.

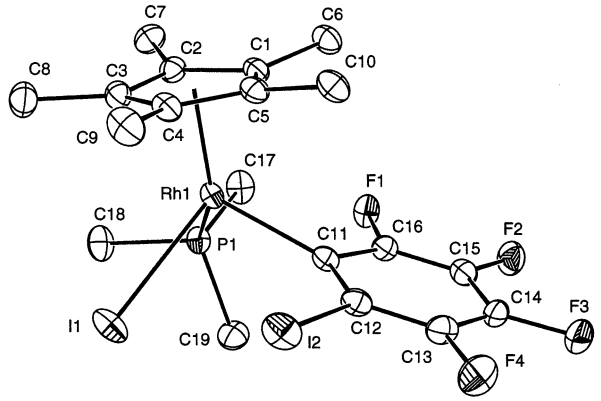

Figure 6. ORTEP plot and atom-numbering scheme for complex **10**. Ellipsoids are shown at the 30% probability level, and H atoms are excluded for clarity.

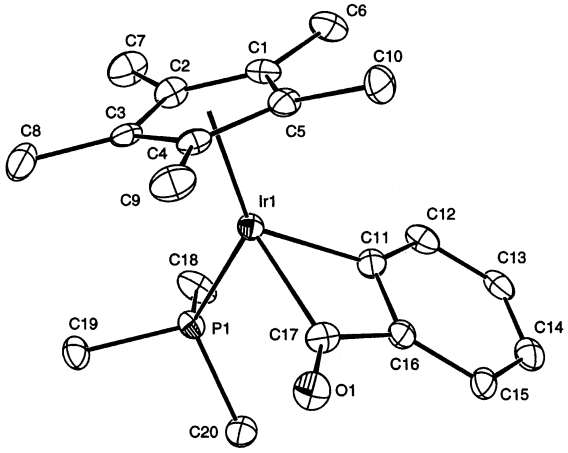

Figure 7. ORTEP plot and atom-numbering scheme for complex **11**. Ellipsoids are shown at the 30% probability level, and H atoms are excluded for clarity. Selected bond distances and angles: Ir1−C11 2.064(8), Ir1−C17 2.084(8), Ir1−P1 2.256(2), O1−C17 1.214(10), C11−C12 1.376(12), C11−C16 1.410(12), C12−C13 1.413(14), C13−C14 1.390(15), C14−C15 1.372(13), C15−C16 1.405(11), C16−C17 1.479(12): O1−C17−C16 128.4(8), O1−C17−Ir1 135.2(7), C12−C11−Ir1 140.8(7), O1−C17−C16 128.4(8).

Experimental Section

All reactions were performed in oven-dried glassware, using standard Schlenk techniques, under an atmosphere of nitrogen, which had been deoxygenated over BASF catalyst and dried over Aquasorb, or in a Braun drybox. Methylene chloride, hexane, diethyl ether, and toluene were dried over an alumina column under nitrogen. IR spectra were recorded on a Perkin-Elmer FTIR 1600 Series spectrometer. NMR spectra were recorded on a Varian Unity Plus 300 or 500 FT spectrometer. ^{1}H NMR spectra were referenced to the protio impurity in the solvent; C_6D_6 (δ 7.16 ppm), $CDCl_3$ (δ 7.27 ppm), CD_2Cl_2 (δ 5.32 ppm). ^{19}F NMR spectra were referenced to $CFCl_3$ (0.00 ppm), and ^{31}P{^{1}H} NMR spectra were referenced to 85% H_3PO_4 (0.00 ppm). Coupling constants are reported in hertz. Elemental analyses were performed by Schwartzkopf (Woodside, NY). Starting complexes **1a**−**c** were prepared as described previously.[11,12]

Cp*Ir(2,3,4,5-C_6F_4H)(PMe_3)(O_2CMe) (2). To a solution of Cp*Ir(η^2-C_6F_4)(PMe_3) (**1a**, 194 mg, 0.352 mmol) in toluene (20 mL) was added $MeCO_2H$ (0.2 mL, 3.49 mmol). The resultant yellow solution was allowed to stir for 1 min, and then the solvent was removed in vacuo to afford a brown oil. A crystalline dull yellow solid was obtained by slow evaporation of a hexane solution. Yield: 136 mg, 63%. Anal. Calcd for $C_{21}H_{28}F_4IrO_2P$: C, 41.24; H, 4.61. Found: C, 41.61; H, 4.78. ^{1}H NMR ($CDCl_3$, 300 MHz, 21 °C): δ 1.38 (d, $^2J_{HP}$ = 10.8 Hz, 9H, PMe_3), 1.63 (d, $^4J_{HP}$ = 1.8 Hz, 15H, Cp*), 7.35 (ddddd, $^3J_{HF}$ = 12.4 Hz, $^4J_{HF}$ = 9.9 Hz, $^5J_{HF}$ = 3.1 Hz, $^4J_{HF}$ = ∼2 Hz, $^4J_{HP}$ = 1.2 Hz, 1H, C_6F_4H). ^{19}F NMR ($CDCl_3$, 282.2 MHz, 21 °C): δ −165.8 (ddd, $^3J_{FF}$ = 21 Hz, $^3J_{FF}$ = 19 Hz, $^4J_{FH}$ = 10 Hz, *p*-C_6F_4H), −160.6 (ddd, $^3J_{FF}$ = 30 Hz, $^3J_{FF}$ = 19 Hz, $^5J_{FH}$ = 3.1 Hz, *m*-C_6F_4H), −143.8 (ddd, $^3J_{FF}$ = 21 Hz, $^5J_{FF}$ = 14 Hz, $^3J_{FH}$ = 12 Hz, *m*-C_6F_4H), −116.3 (dd, $^3J_{FF}$ = 30 Hz, $^5J_{FF}$ = 14 Hz, *o*-C_6F_4H). ^{31}P{^{1}H}NMR ($CDCl_3$, 121.4 MHz, 21 °C): δ −32.8 (PMe_3).

Cp*Ir(2,3,4,5-C_6F_4H)(PMe_3)H (3). To a mixture of Cp*Ir(2,3,4,5-C_6F_4H)(PMe_3)(O_2CMe) (**2**, 75 mg, 0.123 mmol) and $NaBH_4$ (0.2 g, 5.3 mmol) was added EtOH (15 mL), and the resultant yellow solution stirred for 1 h. The volatiles were removed in vacuo, and the solid residue was extracted into hexanes and filtered. Removal of solvent gave an off-white solid. Yield: 67 mg, 98%. X-ray quality crystals were grown by storage of a concentrated solution in hexanes at −30 °C. Anal. Calcd for $C_{19}H_{26}F_4IrP$: C, 41.22; H, 4.73. Found: C, 41.28; H, 4.80. The compound exists in solution as two rotamers in a ratio of 2.3:1. Major rotamer **3a**: ^{1}H NMR (CD_2Cl_2, 300 MHz, −40 °C): δ −17.30 (d, $^2J_{HP}$ = 35.5 Hz, 1H, IrH), 1.32 (d, $^2J_{HP}$ = 10.5 Hz, 9H, PMe_3), 1.83 (d, $^4J_{HP}$ = 1.5 Hz, 15H, Cp*), 7.10 (ddm, $^3J_{HF}$ = 12.7 Hz, $^4J_{HF}$ = 9.9 Hz, 1H, C_6F_4H). ^{19}F NMR (CD_2Cl_2, 282.2 MHz, −40 °C): δ −167.1 (ddd, $^3J_{FF}$ = 22 Hz, $^3J_{FF}$ = 19 Hz, $^4J_{FH}$ = 10 Hz, *p*-C_6F_4H), −160.1 (dd, $^3J_{FF}$ = 34 Hz, $^3J_{FF}$ = 19 Hz, *m*-C_6F_4H), −145.2 (ddd, $^3J_{FF}$ = 22 Hz, $^5J_{FF}$ = 14 Hz, $^3J_{FH}$ = 13 Hz, *m*-C_6F_4H), −112.6 (dd, $^3J_{FF}$ = 34 Hz, $^5J_{FF}$ = 14 Hz, *o*-C_6F_4H). ^{31}P{^{1}H}NMR (CD_2Cl_2, 121.4 MHz, −40 °C): δ −38.1 (d, $^4J_{PF}$ = 5 Hz, PMe_3). Minor rotamer (**3b**): ^{1}H NMR (CD_2Cl_2, 300 MHz, −40 °C): δ −16.54 (dd, $^2J_{HP}$ = 37.5 Hz, $^4J_{HF}$ = 12.5 Hz, 1H, IrH), 1.29 (d, $^2J_{HP}$ = 10.0 Hz, 9H, PMe_3), 1.83 (d, $^4J_{HP}$ = 1.5 Hz, 15H, Cp*), 6.84 (ddm, $^3J_{HF}$ = 12.7 Hz, $^4J_{HF}$ = 8.9 Hz, 1H, C_6F_4H). ^{19}F NMR (CD_2Cl_2, 282.2 MHz, −40 °C): δ −167.3 (ddd, $^3J_{FF}$ = 22 Hz, $^3J_{FF}$ = 20 Hz, $^4J_{FH}$ = 9 Hz, *p*-C_6F_4H), −159.2 (dd, $^3J_{FF}$ = 32 Hz, $^3J_{FF}$ = 20 Hz, *m*-C_6F_4H), −145.3 (ddd, $^3J_{FF}$ = 22 Hz, $^5J_{FF}$ = 13 Hz, $^3J_{FH}$ = 13 Hz, *m*-C_6F_4H), −109.1 (ddd, $^3J_{FF}$ = 32 Hz, $^5J_{FF}$ = 13 Hz, $^4J_{FH}$ = 12.5 Hz, *o*-C_6F_4H). ^{31}P{^{1}H} NMR (CD_2Cl_2, 121.4 MHz, −40 °C): δ −35.8 (s, PMe_3).

Cp*Ir(η^2-3,4,5-C_6F_3H)(PMe_3) (4). To a solution of Cp*Ir(2,3,4,5-C_6F_4H)(PMe_3)H (**3**, 102 mg, 0.184 mmol) in hexanes (15 mL) at −78 °C was added a solution of *n*-BuLi in hexanes (0.66 mL, 2.8 M, 1.8 mmol). The resultant yellow solution was allowed to warm to room temperature and was stirred for 24 h to give an orange cloudy solution. Cooling in an ice-bath, followed by addition of ca. 1 mL of MeOH, and then removal of volatiles in vacuo gave a yellow solid, which was extracted into hexanes and filtered. Removal of solvent from the filtrate in vacuo gave an off-white oily solid, which was recrystallized by slow evaporation of a hexane solution. Yield: 38 mg, 38%. Anal. Calcd for $C_{19}H_{25}F_3IrP$: C, 42.77; H, 4.72. Found: C, 42.76; H, 4.66. ^{1}H NMR (C_6D_6, 300 MHz, 21 °C): δ 0.71 (d, $^2J_{HP}$ = 10.2 Hz, 9H, PMe_3), 1.68 (d, $^4J_{HP}$ = 1.8 Hz, 15H, Cp*), 6.95 (dddd, $^3J_{HF}$ = 2.8 Hz, $^4J_{HF}$ = 3.4 Hz, $^5J_{HF}$ = 3 Hz, $^4J_{HP}$ = 1.2 Hz, 1H, C_6F_3H). ^{19}F NMR (C_6D_6, 282.2 MHz, 21 °C): δ −161.2 (ddd, $^3J_{FF}$ = 29.0 Hz, $^3J_{FF}$ = 10.7 Hz, $^5J_{FH}$ = 3.4 Hz, *m*-C_6F_3H), −141.1 (d, $^3J_{FF}$ = 29 Hz, *o*-C_6F_3H), −136.7 (dd, $^3J_{FF}$ = 10.7 Hz, $^3J_{FH}$ = 2.8 Hz, *m*-C_6F_3H). ^{31}P{^{1}H}NMR (C_6D_6, 121.4 MHz, 21 °C): δ −37.7 (PMe_3).

Cp*Ir(2,3,4-$C_6F_3H_2$)(PMe_3)(O_2CMe) (5)/Cp*Ir(3,4,5-$C_6F_3H_2$)(PMe_3)(O_2CMe) (6). To a solution of Cp*Ir(η^2-3,4,5-C_6F_3H)(PMe_3) (**4**, 38 mg, 0.071 mg) in toluene (5 mL) was added $MeCO_2H$ (0.1 mL, 1.7 mmol). The yellow solution was stirred for 20 min and then the solvent removed in vacuo to afford a yellow oily solid. Yield: 38 mg, 92% (both isomers). The product, which was a mixture of **5** and **6** in a ratio of 8:1, was recrystallized by slow evaporation of a hexane solution. Anal. Calcd for $C_{21}H_{29}F_3IrO_2P$: C, 42.49; H, 4.92. Found: C, 42.63; H, 5.05. **5**: ^{1}H NMR ($CDCl_3$, 500 MHz, 21 °C): δ 1.38

Table 2. Selected Distances (Å) and Angles (deg) for Aryl Complexes 3, 5, 7, 8, and 10

	3	5	7	8	10
M−C(aromatic)	2.062(3)	2.067(5)	2.101(4)	2.122(6)	2.112(3)
M−P	2.2384(8)	2.2822(14)	2.2887(11)	2.2987(17)	2.995(13)
M−X		2.120(3)	2.5522(5)	2.7168(5)	2.7005(12)
M−Ct(01)[a]	1.889(5)	1.846(5)	1.860(5)	1.864(5)	1.864(5)
Ct(01)−M−C	126.56(11)	124.54(11)	121.83(12))	121.82(10)	121.44(10)
Ct(01)−M−P	134.19(12)	130.86(11)	129.10(12)	127.89(10)	127.11(11)
Ct(01)−M−X		130.72(11)	123.29(11)	123.34(11)	123.09(11)
C−M−P(1)	88.84(8)	90.58(14)	93.88(12)	94.61(18)	95.40(9)
C−M−X		87.40(17)	94.46(12)	95.31(17)	96.37(8)
P−M−X		77.19(11)	83.75(3)	83.79(5)	83.87(2)
P−F(*ortho*)[b]	3.66	3.26	2.99	2.97	2.97

[a] Ct(01) = centroid of Cp* ring. [b] Distance from P to the proximal *ortho*-fluorine on the aryl ring.

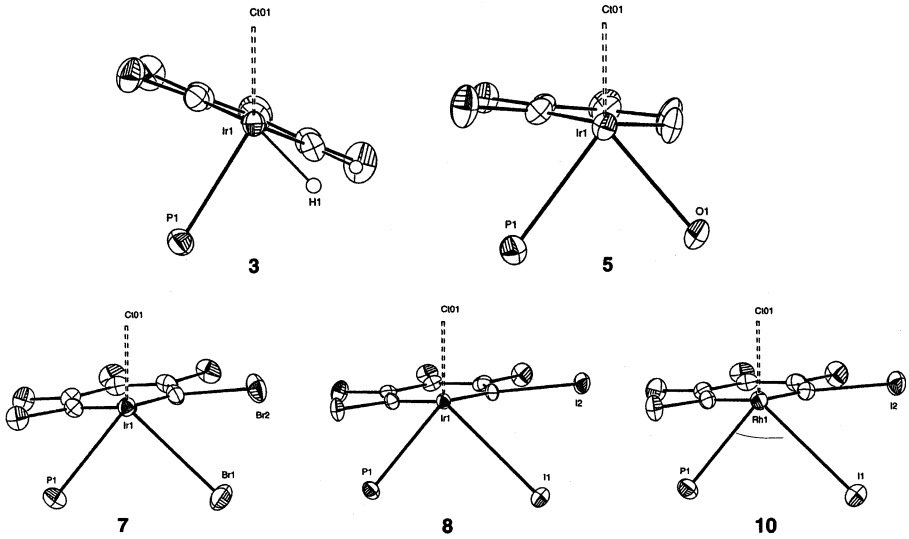

Figure 8. Projections viewed down the M−C bond to the aryl ligand for the aryl complexes **3**, **5**, **7**, **8**, and **10**. Ellipsoids are shown at the 30% probability level, and Cp* carbon atoms, hydrogen atoms, and phosphorus methyl groups are excluded for clarity.

(d, $^2J_{HP}$ = 10.5 Hz, 9H, PMe_3), 1.63 (d, $^4J_{HP}$ = 2.0 Hz, 15H, Cp*), 2.05 (s, 3H, OAc), 6.79 (dddd, $^3J_{HF}$ = 10.0 Hz, $^3J_{HH}$ = 8.7 Hz, $^4J_{HF}$ = 7.0 Hz, $^5J_{HF}$ = 2.0 Hz, 1H, *m*-$C_6H_2F_3$), 7.33 (ddddd, $^3J_{HH}$ = 8.7 Hz, $^4J_{HF}$ = 6.8 Hz, $^4J_{HF}$ = 5.1 Hz, $^5J_{HF}$ = 2.7 Hz, $^4J_{HP}$ = 1.3 Hz, 1H, *o*-$C_6H_2F_3$). ^{19}F NMR ($CDCl_3$, 282.2 MHz, 21 °C): δ −165.3 (dddd, $^3J_{FF}$ = 28.8 Hz, $^3J_{FF}$ = 18.1 Hz, $^4J_{FH}$ = 7.0 Hz, $^5J_{FH}$ = 2.7 Hz, *m*-C_6F_4H), −146.6 (dddd, $^3J_{FF}$ = 18.1 Hz, $^3J_{FH}$ = 10.0 Hz, $^4J_{FH}$ = 6.8 Hz, $^4J_{FF}$ = 4.6 Hz, *p*-C_6F_4H), −112.8 (br, d, $^3J_{FF}$ = 28.8 Hz, *o*-C_6F_4H). ^{31}P{^{1}H} NMR ($CDCl_3$, 121.4 MHz, 21 °C): δ −32.0 (PMe_3). **6**: ^{1}H NMR ($CDCl_3$, 500 MHz, 21 °C): δ 1.36 (d, $^2J_{HP}$ = 10.5 Hz, 9H, PMe_3), 1.58 (d, $^4J_{HP}$ = 2.0 Hz, 15H, Cp*), 2.10 (s, 3H, OAc), 7.10 (br, t, $^3J_{HF}$ = 8 Hz, 2H, $C_6H_2F_3$). ^{19}F NMR ($CDCl_3$, 282.2 MHz, 21 °C): δ −171.9 (tt, $^3J_{FF}$ = 20.0 Hz, $^4J_{FH}$ = 8.0 Hz, *p*-$C_6H_2F_3$), −141.4 (br, s, *m*-$C_6H_2F_3$). ^{31}P{^{1}H}NMR ($CDCl_3$, 121.4 MHz, 21 °C): δ −31.5 (PMe_3).

Reaction of 5/6 with Trifluoroacetic Acid. In an NMR tube, a solution of a mixture of complexes **5** and **6**, prepared as above, was treated with a 10-fold excess of CF_3CO_2H. Monitoring of the solution showed disappearance of the resonances of **5** within 5 min, while the resonances of **6** remained for 24 h. The only organic product was 1,2,3-$C_6F_3H_3$, identified by its NMR spectrum.[14] Removal of the solvent afforded Cp*Ir(O_2CCF_3)$_2$(PMe_3) as a yellow solid. Anal. Calcd for $C_{17}H_{24}F_6IrO_4P$: C, 32.43; H, 3.84. Found: C, 32.38; H, 3.82. ^{1}H NMR (CD_2Cl_2, 300 MHz, 21 °C): δ 1.56 (d, $^2J_{HP}$ = 11.1 Hz, 9H, PMe_3), 1.64 (d, $^4J_{HP}$ = 2.1 Hz, 15H, Cp*). ^{19}F NMR (CD_2Cl_2, 282.2 MHz, 21 °C): δ −75.3 (s, CF_3). ^{31}P{^{1}H} NMR (CD_2Cl_2, 121.4 MHz, 21 °C): δ −14.8.

Cp*Ir(2-C_6BrF_4)(PMe_3)Br (7). To a solution of Cp*Ir(η^2-C_6F_4)(PMe_3) (**1a**, 6.0 mg, 0.011 mmol) in CD_2Cl_2 (0.6 mL) was added Br_2 (0.8 μL, 0.016 mmol). The volatiles were removed in vacuo, and the solid residue was recrystallized from CH_2Cl_2/heptane to afford orange crystals. Yield: 7 mg, 90%. Anal. Calcd for $C_{19}H_{24}Br_2F_4IrP$: C, 32.08; H, 3.40. Found: C, 32.20; H, 3.44. The compound exists in solution as a mixture of two isomers in a ratio of 9:1 at 35 °C. Major isomer **7a**: ^{1}H NMR (CD_2Cl_2, 500 MHz, 35 °C): δ 1.65 (dd, $^2J_{HP}$ = 10.5 Hz, $^6J_{HF}$ = 1.5 Hz, 9H, PMe_3), 1.72 (d, $^4J_{HP}$ = 2.0 Hz, 15H, Cp*); (CD_2Cl_2, 500 MHz, −80 °C) δ 1.25 (d, $^2J_{HP}$ = 11 Hz, 3H, PMe), 1.63 (d, $^4J_{HP}$ = 2.0 Hz, 15H, Cp*), 1.68 (d, $^2J_{HP}$ = 10.5 Hz, 3H, PMe), 1.73 (dd, $^2J_{HP}$ = 9.5 Hz, $^6J_{HF}$ = 3.5 Hz, 3H, PMe). ^{19}F NMR (CD_2Cl_2, 470.3 MHz, 21 °C): δ −160.8 (dd, $^3J_{FF}$ = 22.6 Hz, $^3J_{FF}$ = 19.7 Hz, *p*-C_6F_4Br), −159.1 (dd, $^3J_{FF}$ = 32.4 Hz, $^3J_{FF}$ = 19.7 Hz, *m*-C_6F_4Br), −120.9 (dd, $^3J_{FF}$ = 22.6 Hz, $^5J_{FF}$ = 8.9 Hz, *m*-C_6F_4Br), −100.2 (ddd, $^3J_{FF}$ = 32.4 Hz, $^4J_{FP}$ = 31.4 Hz, $^5J_{FF}$ = 8.9 Hz, *o*-C_6F_4Br). ^{31}P{^{1}H}NMR (CD_2Cl_2, 121.4 MHz, 21 °C): δ −36.7 (d, $^4J_{PF}$ = 31.7 Hz, PMe_3).

Minor isomer **7b**: ^{1}H NMR (CD_2Cl_2, 500 MHz, 35 °C): δ 1.70 (d, $^4J_{HP}$ = 2.0 Hz, 15H, Cp*). PMe_3 signals not observed. ^{19}F NMR (CD_2Cl_2, 470.3 MHz, 21 °C): δ −158.2 (dd, $^3J_{FF}$ = 28.2 Hz, $^3J_{FF}$ = 19.3 Hz, *m*-C_6F_5), −122.5 (dd, $^3J_{FF}$ = 22.1 Hz, $^5J_{FF}$ = 8.9 Hz, *m*-C_6F_5), −94.2 (dd, $^3J_{FF}$ = 28.2 Hz, $^5J_{FF}$ = 8.9 Hz, *o*-C_6F_5). *para*-C_6F_4Br fluorine resonance obscured. ^{31}P{^{1}H} NMR (CD_2Cl_2, 121.4 MHz, 21 °C): δ −40.6 (s, PMe_3).

Cp*Ir(2-C_6IF_4)(PMe_3)I (8). To a solution of Cp*Ir(η^2-C_6F_4)(PMe_3) (**1a**, 6.6 mg, 0.012 mmol) in CD_2Cl_2 (0.3 mL) in an NMR tube was added a solution of I_2 (3.0 mg, 0.012 mmol) in CD_2Cl_2 (0.3 mL). A yellow solution was obtained. NMR spectroscopy showed quantitative conversion to the desired product. Orange crystals were obtained by removal of solvent and recrystallization from CH_2Cl_2/heptane. Anal. Calcd for $C_{19}H_{24}I_2F_4IrP$: C, 28.34; H, 3.00. Found: C, 28.44; H, 2.75. ^{1}H NMR (CD_2Cl_2, 500 MHz, 21 °C): δ 1.76 (br, 9H, PMe_3), 1.81 (d, $^4J_{HP}$ =

2.5 Hz, 15H, Cp*); (CD_2Cl_2, 500 MHz, −75 °C) δ 1.38 (d, $^2J_{HP}$ = 10.5 Hz, 3H, PMe), 1.73 (s, br, 15H, Cp*), 1.76 (dd, $^2J_{HP}$ = 9.5 Hz, $^6J_{HF}$ = 5.5 Hz, 3H, PMe), 1.88 ($^2J_{HP}$ = 10 Hz, 3H, PMe). ^{19}F NMR (CD_2Cl_2, 282.2 MHz, 21 °C): δ −162.0 (dd, $^3J_{FF}$ = 24.8 Hz, $^3J_{FF}$ = 19.2 Hz, *p*-C_6F_4I), −159.7 (dd, $^3J_{FF}$ = 32.2 Hz, $^3J_{FF}$ = 19.2 Hz, *m*-C_6F_4I), −101.7 (dd, $^3J_{FF}$ = 24.8 Hz, $^5J_{FF}$ = 9.0 Hz, *m*-C_6F_4I), −96.4 (ddd, $^3J_{FF}$ = 32.2 Hz, $^4J_{FP}$ = 38.3 Hz, $^5J_{FF}$ = 9.0 Hz, *o*-C_6F_4I). ^{31}P{^{1}H} NMR (CD_2Cl_2, 121.4 MHz, 21 °C): δ −43.2 (d, $^4J_{PF}$ = 38.3 Hz, PMe_3).

Cp*Rh(2-C_6IF_4)(PMe_3)I (9). To a solution of Cp*Rh(η^2-C_6F_4)(PMe_3) (**1b**, 35 mg, 0.076 mmol) in CH_2Cl_2 (10 mL) was added a solution of I_2 (19 mg, 0.075 mmol) in CH_2Cl_2 (1 mL). The solvent was removed in vacuo to give a purple solid. The solid was then dissolved in toluene and passed through a column (silica, toluene). The first, yellow band was discarded, and the second, red band was collected. The solvent was removed in vacuo and the residual solid recrystallized from CH_2Cl_2/heptane to give purple crystals. Yield: 20 mg, 37%. Anal. Calcd for $C_{19}H_{24}F_4I_2PRh$: C, 31.87; H, 3.38. Found: C, 32.01; H, 3.26. ^{1}H NMR ($CDCl_3$, 300 MHz, 21 °C): δ 1.66 (br, d, $^2J_{HP}$ = 9.6 Hz, 9H, PMe_3), 1.79 (d, $^4J_{HP}$ = 3.9 Hz, 15H, Cp*); (CD_2Cl_2, 500 MHz, −75 °C) δ 1.25 (d, $^2J_{HP}$ = 11.0 Hz, 3H, PMe_3), 1.68 (1H, PMe_3 obscured by Cp* resonance), 1.70 (d, $^4J_{HP}$ = 3.0 Hz, 15H, Cp*), 1.80 (d, $^2J_{HP}$ = 10.0 Hz, 3H, PMe_3). ^{19}F NMR ($CDCl_3$, 282.2 MHz, 21 °C): δ − 161.2 (dd, $^3J_{FF}$ = 24.8 Hz, $^3J_{FF}$ = 19.0 Hz, *p*-C_6F_5), −159.2 (dd, $^3J_{FF}$ = 33.3 Hz, $^3J_{FF}$ = 19.0 Hz, *m*-C_6F_5), −101.8 (dd, $^3J_{FF}$ = 24.8 Hz, $^5J_{FF}$ = 9.9 Hz, *m*-C_6F_5), −94.9 (ddm, $^3J_{FF}$ = 33.3 Hz, $^4J_{FP}$ = 48.9 Hz, *o*-C_6F_5). ^{31}P{^{1}H} NMR ($CDCl_3$, 121.4 MHz, 21 °C): δ 0.4 (dd, $^1J_{PRh}$ = 142.8 Hz, $^4J_{PF}$ = 48.9 Hz, PMe_3).

Cp*Ir(2-C_6MeF_4)(PMe_3)I (10). A mixture of Cp*Ir(η^2-C_6F_4)(PMe_3) (**1a**, 6.0 mg, 0.011 mmol) and MeI (0.02 mL, 0.3 mmol) in C_6D_6 (0.7 mL) was heated in an NMR tube at 105 °C for 84 h. NMR spectroscopy showed quantitative conversion to the desired product. The product was obtained in crystalline form by removal of solvent and recrystallization from CH_2Cl_2/heptane, yielding orange crystals. Anal. Calcd for $C_{20}H_{27}F_4IIrP$: C, 34.64; H, 3.92. Found: C, 34.93; H, 3.66. ^{1}H NMR ($CDCl_3$, 300 MHz, 21 °C): δ 1.76 (d, $^4J_{HP}$ = 2.4 Hz, 15H, Cp*) 1.77 (dd, $^2J_{HP}$ = 9.6 Hz, $^6J_{HF}$ = 2.1 Hz, 9H, PMe_3) 2.45 (dd, $^4J_{HF}$ = 5.4 Hz, $^5J_{HF}$ = 1.5 Hz, 3H, C_6F_4*Me*). ^{19}F NMR ($CDCl_3$, 282.2 MHz, 21 °C): δ − 165.7 (dd, $^3J_{FF}$ = 21.4 Hz, $^3J_{FF}$ = 19.8 Hz, *p*-C_6F_4Me), −164.0 (dd, $^3J_{FF}$ = 32.5 Hz, $^3J_{FF}$ = 19.8 Hz, *m*-C_6F_4Me), −138.4 (ddq, $^3J_{FF}$ = 21.4 Hz, $^5J_{FF}$ = 10.4 Hz, $^4J_{FH}$ = 5.4 Hz, *m*-C_6F_4Me), −106.0 (ddd, $^3J_{FF}$ = 32.5 Hz, $^4J_{FP}$ = 33.9 Hz, $^5J_{FF}$ = 10.4 Hz, *o*-C_6F_4Me). ^{31}P{^{1}H} NMR ($CDCl_3$, 121.4 MHz, 21 °C): δ −45.0 (d, $^4J_{PF}$ = 33.9 Hz, PMe_3).

Cp*Ir(PMe_3)(C_6H_4CO) (11). A solution of Cp*Ir(PMe_3)(C_6H_4) (**1c**, 22 mg (0.046 mmol) in dry toluene (10 mL) was placed in a Schlenk flask, and the flask was evacuated and backfilled with CO gas. The resultant pale green solution was stirred for 2 h under reflux, during which time the color of the solution changed to yellow. The mixture was cooled, the solvent removed in vacuo, and the resultant solid crystallized from dry hexanes to give X-ray quality crystals (22 mg; 95%). Anal. Calcd for $C_{30}H_{28}IrOP$: C, 47.32; H, 5.56. Found: C, 47.12; H, 5.24. IR (toluene): 1653, 1697 cm^{-1}. ^{1}H NMR (C_6D_6, 300 MHz, 22 °C): δ 0.96 (d, $^2J_{HP}$ = 9.9 Hz, 9H, PMe_3), 1.74 (d, $^4J_{HP}$ = 1.5 Hz, 15H, Cp*), 6.87 (m, 2H, C_6H_4), 7.20 (m, 2H, C_6H_4). ^{31}P{^{1}H} NMR (C_6D_6, 121.4 MHz, 22 °C): δ −34.72 (s, PMe_3).

Cp*Ir(2-C_6IH_4)(PMe_3)I (12). To a solution of Cp*Ir(PMe_3)(C_6H_4) (**1c**, 33 mg, 0.069 mmol) in dry hexanes (15 mL) was added dropwise a solution of I_2 (17 mg, 0.065 mmol, 0.95 equiv) in dry hexanes (purple). An instantaneous reaction was observed to give an orange saturated solution from which a precipitate formed. The solid was filtered and crystallized from toluene (95%). Anal. Calcd for $C_{29}H_{28}I_2IrP$: C, 31.11; H, 3.85. Found: C, 31.44; H, 3.60. The compound exists as two rotamers about the Ir−C bond in solution. In C_6D_6 the ratio is 12:1, while in CD_2Cl_2 it is 5:1.

Major rotamer: ^{1}H NMR (C_6D_6, 500 MHz, 21 °C): δ 1.44 (d, $^4J_{HP}$ = 1.8 Hz, 15H, Cp*), 1.64 (d, $^2J_{HP}$ = 9.9 Hz, 9H, PMe_3), 6.49 (ddd, $^3J_{HH}$ = 7.5 Hz, $^3J_{HH}$ = 7.5 Hz, $^4J_{HH}$ = 1.5 Hz, 1H, C_6H_4I), 6.85 (ddd, $^3J_{HH}$ = 7.5 Hz, $^3J_{HH}$ = 7.5 Hz, $^4J_{HH}$ = 1.5 Hz,1H, C_6H_4I), 7.965 (dd, $^3J_{HH}$ = 7.5 Hz, $^4J_{HH}$ = 1.5 Hz, 1H, C_6H_4I), 8.83 (ddd, $^3J_{HH}$ = 7.5 Hz, $^4J_{HH}$ = 1.5 Hz, $^4J_{HP}$ = 0.75 Hz, 1H, C_6H_4I). ^{31}P{^{1}H} NMR (C_6D_6, 202.4 MHz, 21 °C): δ −49.75 (s, PMe_3). ^{1}H NMR (CD_2Cl_2, 500 MHz, 21 °C): δ 1.70 (d, $^4J_{HP}$ = 1.8 Hz, 15H, Cp*), 1.895 (bd, $^2J_{HP}$ = 9.9 Hz, 9H, PMe_3), 6.445 (ddd, $^3J_{HH}$ = 7.5 Hz, $^3J_{HH}$ = 7.5 Hz, $^4J_{HH}$ = 1.5 Hz, 1H, C_6H_4I), 6.66 (ddd, $^3J_{HH}$ = 7.5 Hz, $^3J_{HH}$ = 7.5 Hz, $^4J_{HH}$ = 1.5 Hz,1H, C_6H_4I), 7.65 (dd, $^3J_{HH}$ = 7.5 Hz, $^4J_{HH}$ = 1.5 Hz, 1H, C_6H_4I), 8.235 (ddd, $^3J_{HH}$ = 7.5 Hz, $^4J_{HH}$ = 1.5 Hz, $^4J_{HP}$ = 0.75 Hz, 1H, C_6H_4I). ^{31}P{^{1}H} NMR (CD_2Cl_2, 202.4 MHz, 21 °C): δ −48.92 (s, PMe_3). ^{1}H NMR (CD_2Cl_2, 500 MHz, −75 °C): δ 1.57 (bd, $^2J_{HP}$ = 11 Hz, 3H, PMe_3), 1.87 (bd, $^2J_{HP}$ = 9 Hz, 3H, PMe_3), 1.97 (bd, $^2J_{HP}$ = 9.5 Hz, 3H, PMe_3)

Minor rotamer: ^{1}H NMR (C_6D_6, 500 MHz, 21 °C): δ 1.49 (d, $^4J_{HP}$ = 1.8 Hz, 15H, Cp*), PMe_3), 6.47 (ddd, 1H, C_6H_4I), 6.79 (ddd, $^3J_{HH}$ = 7.5 Hz, $^3J_{HH}$ = 7.5 Hz, $^4J_{HH}$ = 1.5 Hz, 1H, C_6H_4I), 8.19 (dd, $^3J_{HH}$ = 7.5 Hz, $^4J_{HH}$ = 1.5 Hz, 1H, C_6H_4I), due to overlap of the PMe_3 resonance and one of the aryl resonances could not be observed. ^{31}P{^{1}H} NMR (C_6D_6, 202.4 MHz, 21 °C): δ −41.55 (s, PMe_3). ^{1}H NMR (CD_2Cl_2, 500 MHz, 21 °C): δ 1.76 (d, $^4J_{HP}$ = 1.8 Hz, 15H, Cp*), 6.44 (ddd, 1H, C_6H_4I), 6.80 (ddd, $^3J_{HH}$ = 7.5 Hz, $^3J_{HH}$ = 7.5 Hz, $^4J_{HH}$ = 1.5 Hz, 1H, C_6H_4I), 7.22 (dm, $^3J_{HH}$ = 7.5 Hz, 1H, C_6H_4I), 7.81 (dd, $^3J_{HH}$ = 7.5 Hz, $^4J_{HH}$ = 1.5 Hz, 1H, C_6H_4I), due to overlap of the PMe_3 resonance could not be observed. ^{31}P{^{1}H} NMR (CD_2Cl_2, 202.4 MHz, 21 °C): δ −40.27 (s, PMe_3). ^{1}H NMR (CD_2Cl_2, 500 MHz, −75 °C): δ 1.40 (bd, $^2J_{HP}$ = 11 Hz, 3H, PMe_3), 1.655 (bd, $^2J_{HP}$ = 10 Hz, 3H, PMe_3), 1.85 (bd, overlapping, 3H, PMe_3).

Crystallographic Determinations. Crystal, data collection, and refinement parameters are collected in Table 1. Systematic absences in the diffraction data are uniquely consistent for the reported space groups and yielded chemically reasonable and computationally stable results on refinement. The structures were solved using direct methods, completed by subsequent difference Fourier syntheses, and refined by full-matrix least-squares procedures. SADABS absorption corrections were applied to **3** and **8**, and DIFABS absorption corrections to **4** and **5**.[21] All non-hydrogen atoms were refined with anisotropic displacement coefficients, and hydrogen atoms were treated as idealized contributions.

All software and sources of scattering factors are contained in the SHELXTL program libraries (various versions, G. Sheldrick, Bruker AXS, Madison, WI).

Acknowledgment. R.P.H. is grateful to the National Science Foundation for generous financial support.

Supporting Information Available: Atomic fractional coordinates, bond distances and angles, and anisotropic thermal parameters for complexes **3**, **4**, **5**, **7**, **8, 10**, and **11** are available free of charge via the Internet at http://pubs.acs.org.

OM030048W

(21) Walker, N.; Stuart, D. *Acta Crystallogr. Sect. A* **1983**, *39*, 158−166.